

Comparison of the Interactions of Transferrin Receptor and Transferrin Receptor 2 with Transferrin and the Hereditary Hemochromatosis Protein HFE*

Received for publication, September 22, 2000
Published, JBC Papers in Press, October 10, 2000,
DOI 10.1074/jbc.C000664200

Anthony P. West, Jr.‡, Melanie J. Bennett‡,
Vera M. Sellers§, Nancy C. Andrews§,
Caroline A. Enns¶, and Pamela J. Bjorkman‡||**

From the ‡Division of Biology and ¶Howard Hughes Medical Institute, California Institute of Technology, Pasadena, California 91125, the §Division of Hematology-Oncology, Children's Hospital, Howard Hughes Medical Institute and Department of Pediatrics, Harvard Medical School, Boston, Massachusetts 02115, and the ¶Department of Cell and Developmental Biology, Oregon Health Sciences University, Portland, Oregon 97201-3098

The transferrin receptor (TfR) interacts with two proteins important for iron metabolism, transferrin (Tf) and HFE, the protein mutated in hereditary hemochromatosis. A second receptor for Tf, TfR2, was recently identified and found to be functional for iron uptake in transfected cells (Kawabata, H., Germain, R. S., Vuong, P. T., Nakamaki, T., Said, J. W., and Koeffler, H. P. (2000) *J. Biol. Chem.* 275, 16618–16625). TfR2 has a pattern of expression and regulation that is distinct from TfR, and mutations in TfR2 have been recognized as the cause of a non-HFE linked form of hemochromatosis (Camaschella, C., Roetto, A., Cali, A., De Gobbi, M., Garozzo, G., Carella, M., Majorano, N., Totaro, A., and Gasparini, P. (2000) *Nat. Genet.* 25, 14–15). To investigate the relationship between TfR, TfR2, Tf, and HFE, we performed a series of binding experiments using soluble forms of these proteins. We find no detectable binding between TfR2 and HFE by co-immunoprecipitation or using a surface plasmon resonance-based assay. The affinity of TfR2 for iron-loaded Tf was determined to be 27 nM, 25-fold lower than the affinity of TfR for Tf. These results imply that HFE regulates Tf-mediated iron uptake only from the classical TfR and that TfR2 does not compete for HFE binding in cells expressing both forms of TfR.

Mammalian organisms possess complex mechanisms to regulate the absorption and uptake of iron on both the cellular and

* This work was supported by the Howard Hughes Medical Institute (to P. J. B. and N. C. A.), Grant DRG-1445 from the Cancer Research Fund of the Damon Runyon-Walter Winchell Foundation Fellowship (to A. P. W.), and National Institutes of Health Grant DK 54488 (to C. A. E.). The costs of publication of this article were defrayed in part by the payment of page charges. This article must therefore be hereby marked "advertisement" in accordance with 18 U.S.C. Section 1734 solely to indicate this fact.

** To whom correspondence should be addressed: Division of Biology 156–29, California Inst. of Technology, Pasadena, CA 91125. Tel.: 626-395-8350; Fax: 626-792-3683; E-mail: bjorkman@its.caltech.edu.

organism level. The transferrin receptor (TfR)¹ plays a central role in iron metabolism in which transferrin (Tf)-bound iron is taken up into cells via binding to TfR and endocytosis of the TfR-Tf complex (reviewed in Ref. 1). TfR is a homodimeric membrane glycoprotein that binds two molecules of Tf (1). Upon exposure to the acidic pH of the endosome, iron is released from Tf and enters a chelatable intracellular pool from which it is utilized for the metabolic needs of the cell or incorporated into the storage protein ferritin. Iron-free Tf (apoTf) remains bound to TfR at the low pH value of the acidic vesicle (\leq pH 6.4), and the apoTf-TfR complex is then recycled to the cell surface where apoTf dissociates at the higher pH value of blood (\sim pH 7.4).

In cell lines and in tissues such as the intestine and placenta, TfR associates with HFE, another protein involved in the regulation of iron metabolism (2, 3), and HFE association with TfR has been shown to negatively regulate Tf-mediated iron uptake in transfected cells (4–6). HFE is a class I major histocompatibility complex (MHC)-related protein that is mutated in patients with hereditary hemochromatosis (7), an iron storage disease characterized by excessive iron absorption leading to an accumulation of iron principally in the liver, heart, pancreas, and parathyroid and pituitary glands (8). Like class I MHC molecules, HFE is composed of a heavy chain with three extracellular domains (α 1, α 2, and α 3), a single transmembrane-spanning region, a short cytoplasmic domain, and the non-covalently associated light chain, β 2-microglobulin. Class I MHC proteins bind peptides in a groove within the α 1- α 2 superdomain and present them to T cells as part of the adaptive immune response against pathogens (9). HFE contains a narrowed version of the class I peptide binding groove and does not bind peptides or play any known role in the immune system (10). Instead HFE associates with TfR (2, 3) in a pH-dependent interaction, such that a nanomolar binding affinity is observed at pH 7.5 with no detectable binding at pH 6 and below (10). Crystal structures of HFE (10), TfR (11), and the HFE-TfR complex (12) reveal the molecular basis for the interaction between TfR and HFE and, when combined with biochemical studies, suggest a binding site on TfR for Tf (13).

Recently, a second receptor for Tf, TfR2, was identified (14). Like TfR, it is a type II transmembrane protein consisting of an N-terminal cytoplasmic domain and a large C-terminal ectodomain. Human TfR2 shares 45% amino acid sequence identity in its extracellular region with human TfR. In human and mouse, TfR2 is highly expressed in the liver and in peripheral blood mononuclear cells (15, 16). In contrast to TfR, expression of TfR2 is not down-regulated as a result of iron overload, consistent with the absence of iron-responsive elements in the 3' untranslated sequence of TfR2 mRNA (16). Flow cytometric analyses of Tf binding to TfR2 expressed in a Chinese hamster ovary cell line lacking endogenous TfR demonstrate that TfR2 binds Tf (14). In addition, expression of TfR2 in this cell line permits cell growth in iron-chelated media, demonstrating that TfR2 is functional for Tf-mediated iron uptake (15). A homozygous nonsense mutation in TfR2 has been identified as the cause of a form of hemochromatosis that is not linked to mutations in HFE (17), demonstrating that TfR2 is critical for

¹ The abbreviations used are: TfR, transferrin receptor; Tf, transferrin; MHC, major histocompatibility complex; RU, resonance units; PIPES, 1,4-piperazinediethanesulfonic acid.

maintenance of iron homeostasis, but possible interactions between TfR2 and HFE were not investigated.

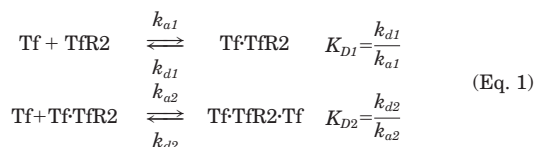
In this communication, we compared the interactions of the ectodomains of TfR2 and TfR with Tf and HFE. We find that Tf binds to TfR2, although more weakly than it binds TfR, but that TfR2 does not interact detectably with HFE. These data imply that HFE exerts its influence on iron homeostasis through interactions with TfR and not TfR2.

EXPERIMENTAL PROCEDURES

Expression and Purification of TfR2—A soluble version of human TfR2 was expressed in a lytic baculovirus/insect cell expression system using the approach described previously for expression of soluble TfR (10). A construct encoding residues 133–801 (the C-terminal amino acid of wild-type TfR2) was joined 3' to a gene segment encoding the leader peptide from the baculovirus protein GP67, a 6xHis-tag, and a factor X_a cleavage site in a modified form of the pAcGP67A expression vector (Pharmingen). Recombinant virus was generated by co-transfection of the transfer vector with linearized viral DNA (Baculogold; Pharmingen). TfR2 was purified from supernatants of baculovirus-infected High 5 cells using nickel-nitrilotriacetic acid chromatography (Ni-NTA Superflow; Qiagen) followed by gel filtration chromatography using a Superdex-200 fast protein liquid chromatography column (Amersham Pharmacia Biotech). The gel filtration step was required to remove aggregated TfR2 that eluted in the void volume of the column and that did not bind Tf. Unaggregated TfR2 eluted in a broad peak at a higher apparent molecular weight than did TfR (data not shown). N-terminal sequencing of purified TfR2 yielded the sequence ADPHHHHHSS-GIEGRGEFGRLYW, which corresponds to the 6xHis-tag, spacer, factor X_a site, and residues 133–137 of TfR2.

Determination of Protein Concentrations—Protein concentrations were determined spectrophotometrically using extinction coefficients at 280 nm of 83360 M⁻¹ cm⁻¹ (Tf), 96570 M⁻¹ cm⁻¹ (HFE), 93790 M⁻¹ cm⁻¹ (TfR), and 93430 M⁻¹ cm⁻¹ (TfR2). Extinction coefficients were calculated as described previously (10).

Biosensor Assays—A BIACORE 2000 biosensor system (Biacore AB) was used to assay the interaction of TfR and TfR2 with HFE and human Tf (Sigma). Tf was further purified by gel filtration chromatography prior to biosensor analyses. The BIACORE system includes a biosensor chip with a dextran-coated gold surface to which one protein (referred to as the “ligand”) is immobilized. Binding of an injected protein (the “analyte”) to the immobilized protein results in changes in surface plasmon resonance that are directly proportional to the amount of bound protein and read out in real time as resonance units (RU) (18, 19). TfR or TfR2 was immobilized using an oriented coupling procedure in which an anti-His-tag antibody (anti-pentahis; Qiagen) was covalently attached to the chip surface followed by injection of the His-tagged protein. The anti-His-tag antibody was coupled (2000–3000 RU) to all four flow cells on a CM5 biosensor chip (Biacore AB) using standard primary amine-coupling chemistry (BIACORE manual). His-tagged TfR or TfR2 was then injected in 50 mM PIPES, pH 7.5, 150 mM NaCl, 0.005% surfactant P20 and allowed to bind to individual flow cells at levels between 200 and 400 RU. Although a small portion of the bound TfR or TfR2 dissociates within a few minutes of this binding step, the majority remains bound, and the baseline does not drift significantly. A flow cell containing only immobilized antibody served as a blank. HFE or Tf was injected over the TfR- or TfR2-coupled flow cells at room temperature in 50 mM PIPES, pH 7.5, 150 mM NaCl, 0.005% surfactant P20. Equilibrium dissociation constants (K_D) were calculated from association and dissociation rate constants, which were derived from binding experiments with 4-min association and 4-min dissociation phases using a flow rate of 50 μl/min. Kinetic constants were calculated from sensorgram data using simultaneous fitting of the association and dissociation phases with global fitting to all curves in the working set using CLAMP 99 (20). The data were fit to a bivalent ligand model, *i.e.*, the two sequential binding steps shown in Equation 1.



Coinmunoprecipitation of HFE with TfR and TfR2—HFE (450 pmol) and TfR (150 pmol) or TfR2 (150 pmol) were incubated for 30 min at room temperature in 20 μl of 20 mM Tris-Cl, 150 mM NaCl, pH 7.5.

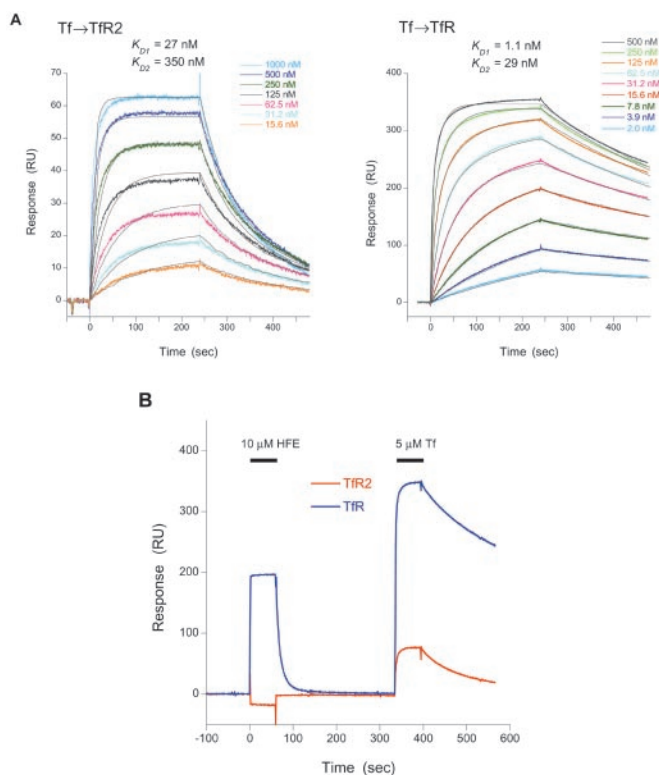


FIG. 1. Biosensor analyses of Tf and HFE binding to immobilized TfR and TfR2. A, sensorgrams (colored curves) of injected Tf binding to TfR2 (left panel) or TfR (right panel) immobilized using a covalently attached anti-His-tagged antibody. Best fit binding curves (assuming a bivalent ligand model) are shown as thin black lines. B, sensorgrams showing injection of 10 μM HFE and 5 μM Tf onto flow cells containing either TfR2 (red) and TfR (blue). Injection duration for HFE and Tf are indicated above the sensorgrams.

Either 2 μg of anti-pentahis antibody (Qiagen) or 2 μg anti-HFE (1C3) (10) antibody were added to the sample as indicated, followed by 30 μl of protein G-Sepharose (Amersham Pharmacia Biotech). The mixture was incubated on a rotating platform for 1 h at room temperature. Samples were layered on top of 1 ml of 20 mM Tris-Cl, 150 mM NaCl, pH 7.5, 15% sucrose and pelleted in a microfuge for 2 min at 14000 × g. The supernatants were aspirated, and the pellets were resuspended in 2× Laemmli buffer. The samples were heated to 95 °C for 3 min, loaded onto an SDS polyacrylamide (10%) gel, and electrophoresed under denaturing and reducing conditions. The experiment was repeated three times with similar results.

RESULTS

Biosensor Assays Using Soluble TfR and TfR2—To investigate the binding properties of TfR2, we expressed a soluble, polyhistidine-tagged form of the TfR2 ectodomain (residues 133–801) and performed a series of affinity measurements using a surface plasmon resonance-based assay. Purified soluble TfR2 was attached to the sensor chip through an anti-His-tagged antibody, and a series of injections of Tf and HFE were performed at pH 7.5. Kinetic analysis of Tf binding to TfR2 (Fig. 1A) yielded two affinities, $K_{D1} = 27$ nM and $K_{D2} = 350$ nM, when the data were fit to a model with stepwise binding of two molecules of Tf to each TfR2 homodimer. Under identical conditions the corresponding Tf affinities for TfR (Fig. 1A) are $K_{D1} = 1.1$ nM and $K_{D2} = 29$ nM, similar to results obtained from previous biosensor- and cell-based measurements of the affinity between TfR and Tf (1, 10). Hence, the affinity of the first Tf binding to TfR2 is about 25-fold lower than the corresponding affinity of Tf for TfR. This is in agreement with cell surface measurements of the Tf affinity for full-length TfR and TfR2, in which a 30-fold difference was observed (15).

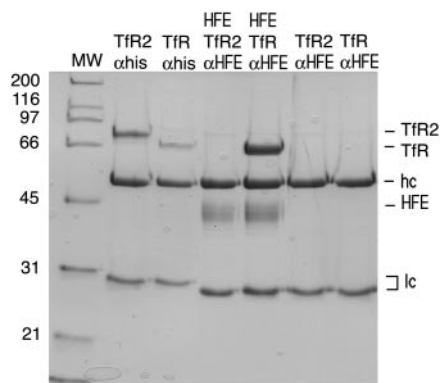


FIG. 2. **HFE does not immunoprecipitate with Tfr2.** Coomassie blue-stained SDS polyacrylamide (10%) gel of immunoprecipitation of HFE in the presence of Tfr or Tfr2 is shown. HFE was incubated with Tfr or Tfr2 at pH 7.5 for 30 min at room temperature. Immunoprecipitations were performed with either the anti-pentahis antibody or an anti-HFE antibody. The mobilities of Tfr2, Tfr, HFE, and the antibody heavy chains (*hc*) and light chains (*lc*) are denoted in the *right-hand margin*. The HFE light chain, β 2-microglobulin, is present on gels composed of a higher percentage of acrylamide (data not shown). The experiment was repeated three times with similar results.

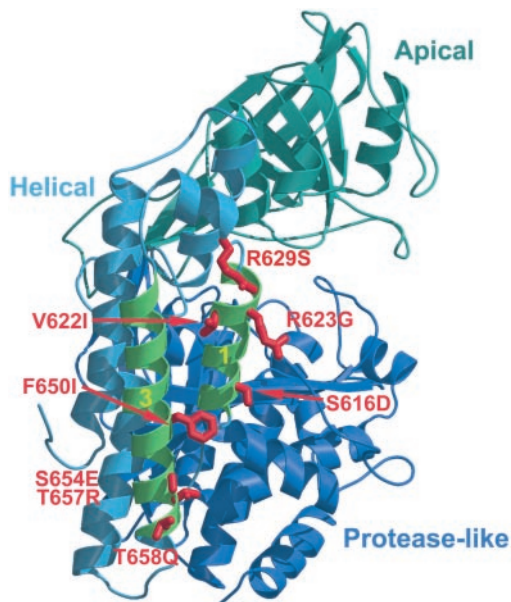


FIG. 3. **Tfr2 amino acid substitutions in the HFE-binding site mapped onto Tfr structure.** Ribbon diagram of one polypeptide chain of the Tfr homodimer derived from the 2.8-Å HFE-Tfr complex structure (12) shown with the two helices that interact with HFE highlighted in *green* (helical domain helices 1 and 3). Tfr residues that are involved in binding HFE and substituted in Tfr2 are shown in *red*.

We next examined the ability of Tfr2 to bind HFE, using Tfr as a positive control. The affinity of soluble HFE for immobilized Tfr is ~ 300 nM (10), and binding can be observed at concentrations as low as 20 nM. However, for Tfr2, injections of HFE at concentrations up to $10 \mu\text{M}$ did not lead to detectable binding (Fig. 1B), implying a $K_D \gg 10 \mu\text{M}$. These HFE injections were performed on Tfr2 samples that were competent to bind Tf and under conditions in which HFE binding to Tfr was easily observed (Fig. 1B). We previously demonstrated that a $K_D > 9 \mu\text{M}$ derived from the interaction of a soluble mutant HFE with soluble Tfr is insufficient to confer an interaction in the cell between membrane-bound forms of these proteins (21). We therefore assume that binding between membrane HFE

TABLE I

HFE-interacting residues on Tfr and their counterparts in Tfr2

HFE-interacting residues on Tfr were identified from the 2.8-Å resolution HFE-Tfr complex structure as described (12). Corresponding residues in Tfr2 are listed based on the sequence alignment in Ref. 14 with differences indicated in bold lettering. The number of hydrogen bonds (in parentheses) and % accessible surface area were calculated using the protein-protein interactions server (24). % Accessible surface area, percent of total interface area contributed by each Tfr residue; vdW, interactions with HFE involving only van der Waals interactions; H bond, interactions with HFE that include hydrogen bonds.

Tfr residue	Tfr2 residue	% Accessible with HFE	Type of interaction
Ser-616	Asp-648	3	vdW
Leu-619	Leu-651	10	vdW
Val-622	Ile-654	2	vdW
Arg-623	Gly-655	7	vdW
Asn-626	Asn-656	5	vdW
Arg-629	Ser-661	10	H bonds (4)
Gln-640	Gln-672	10	H bond (1)
Trp-641	Trp-673	5	vdW
Tyr-643	Tyr-675	4	vdW
Ser-644	Ser-676	4	vdW
Arg-646	Arg-678	5	vdW
Asp-648	Asp-680	1	H bond (1)
Phe-650	Ile-682	7	vdW
Arg-651	Arg-683	5	vdW
Ser-654	Glu-686	5	vdW
Thr-657	Arg-689	4	vdW
Thr-658	Gln-690	4	H bond (1)

and Tfr2 is unlikely, even when both proteins are tethered to the same membrane.

Immunoprecipitations—As independent verification of the biosensor analysis demonstrating that HFE and Tfr2 do not interact, we also tested whether Tfr2 could be coimmunoprecipitated with HFE using an anti-HFE monoclonal antibody. As shown in Fig. 2, Tfr, but not Tfr2, coimmunoprecipitates with HFE. These experiments were done at an HFE concentration of $9 \mu\text{M}$, implying the K_D for the Tfr2-HFE interaction is higher than $9 \mu\text{M}$.

DISCUSSION

Here we report the expression and characterization of a soluble version of Tfr2 analogous to soluble Tfr, whose interactions with Tf and HFE were previously described (10). Using a quantitative biosensor-based assay, we find that the affinity of Tf for soluble Tfr2 is ~ 25 -fold lower than that for Tfr. Both biosensor and immunoprecipitation experiments fail to detect any interaction between the ectodomains of HFE and Tfr2, implying a $K_D \gg 10 \mu\text{M}$, which should be insufficient to confer an interaction between membrane-bound forms of the molecules (21).

The Tfr structural features that are involved in binding HFE have been determined from a crystallographic structure of the HFE-Tfr complex at 2.8-Å resolution (12). The structure shows that two helices in the helical domain of Tfr (helical domain helices 1 and 3) (Fig. 3) interact with the HFE α 1 and α 2 domain helices, forming an extensive interface. The interface includes both apolar and polar interactions and buries 1000 \AA^2 of solvent-accessible surface area per subunit. About half of the Tfr residues that form contacts with HFE are replaced by different amino acids in Tfr2 (see Fig. 3 and Table I), suggesting a structural interpretation for the lack of HFE binding by Tfr2. Although some critical binding residues are identical (*e.g.* Tfr Leu-619) or conservatively replaced (*e.g.* Tfr Val-622 *versus* Tfr2 Ile-654), some substitutions in Tfr2 are likely to be incompatible with HFE binding. For example, several replacements significantly reduce the buried surface area in the interface (*e.g.* Tfr Arg-623 *versus* Tfr2 Gly-655). Several

other substitutions replace small polar residues (serine or threonine) with charged residues (*e.g.* TfR Ser-654 *versus* TfR2 Glu-686). Other substitutions would disrupt the hydrogen bond network in the interface (*e.g.* TfR Arg-629 *versus* TfR2 Ser-661). These changes in TfR2 would be expected to destabilize the interaction with HFE.

TfR2 and TfR can both bind Tf, suggesting that they share a similar Tf-binding site. There is no crystal structure for a TfTfR complex; however some features of the Tf-binding site in TfR can be inferred from biochemical studies and knowledge of the structures of TfR (11) and the TfR·HFE complex (12). Competition studies demonstrate that HFE and Tf bind to an overlapping site on TfR (13); therefore some of the HFE-interacting residues in TfR must also contribute to the Tf-binding site (Table I). In support of this idea, site-directed mutagenesis has shown that TfR residues 646–648, which are present at the HFE-binding site, are critical for Tf binding (22). Residues 646–648 are conserved in TfR2 and are therefore likely to be involved in the TfR2 interaction with Tf (Table I). Similarly, other HFE-interacting residues that are conserved between TfR2 and TfR may contribute to the Tf-binding site.

HFE competes with Tf for binding to TfR (13) and reduces cellular iron levels in cells expressing both HFE and TfR (4–6, 21, 23). Here we demonstrate that HFE does not bind to TfR2 and thus would not be expected to regulate TfR2-mediated iron uptake. Curiously, for both HFE and TfR2, the mechanism whereby mutation of either protein leads to hemochromatosis remains unclear. How does the absence of HFE and subsequent increased cellular iron absorption by TfR on the basolateral side of the intestinal crypt cell lead to increased iron transport across the enterocyte? In addition, how does the absence of TfR2 in liver and erythroid cells cause intestinal cells to sense iron deficiency despite the body's state of iron overload? These questions remain to be answered, but the recent finding that TfR2 is mutated in a non-HFE-related form of hemochromatosis (17) implies that TfR2 must be included in any models for the regulation of iron homeostasis. Our demonstration that HFE does not bind to TfR2 implies that TfR2 cannot compete for HFE binding in cells expressing both forms of TfR and is consistent with the emerging picture that TfR and TfR2 are regulated in distinct ways.

Acknowledgments—We thank Dr. Peter Snow of the Caltech Protein Expression Facility for construction of recombinant baculovirus expressing TfR2 and Dr. Andrew Herr for help with biosensor analyses.

REFERENCES

- Richardson, D. R., and Ponka, P. (1997) *Biochim. Biophys. Acta* **1331**, 1–40
- Feder, J. N., Penny, D. M., Irrinki, A., Lee, V. K., Lebrón, J. A., Watson, N., Tsuchihashi, Z., Sigal, E., Bjorkman, P. J., and Schatzman, R. C. (1998) *Proc. Natl. Acad. Sci. U. S. A.* **95**, 1472–1477
- Parkkila, S., Waheed, A., Britton, R. S., Bacon, B. R., Zhou, X. Y., Tomatsu, S., Fleming, R. E., and Sly, W. S. (1997) *Proc. Natl. Acad. Sci. U. S. A.* **94**, 13198–13202
- Gross, C. N., Irrinki, A., Feder, J. N., and Enns, C. A. (1998) *J. Biol. Chem.* **273**, 22068–22074
- Roy, C. N., Penny, D. M., Feder, J. N., and Enns, C. A. (1999) *J. Biol. Chem.* **274**, 9022–9028
- Corsi, B., Levi, S., Cozzi, A., Corti, A., Altimare, D., Albertini, A., and Arosio, P. (1999) *FEBS Lett.* **460**, 149–152
- Feder, J. N., Gnirke, A., Thomas, W., Zsuzihashi, Z., Ruddy, D. A., Basava, A., Dormishian, F., Domingo, R., Ellis, M. C., Fullan, A., Hinton, L. M., Jones, N. L., Kimmel, B. E., Kronmal, G. S., Lauer, P., Lee, V. K., Loeb, D. B., Mapa, F. A., McClland, E., Meyer, N. C., Mintier, G. A., Moeller, N., Moore, T., Morikang, E., Prass, C. E., Quintana, L., Starnes, S. M., Schatzman, R. C., Brunke, K. J., Drayna, D. T., Risch, N. J., Bacon, B. R., and Wolff, R. K. (1996) *Nat. Genet.* **13**, 399–408
- Cullen, L. M., Anderson, G. J., Ramm, G. A., Jazwinska, E. C., and Powell, L. W. (1999) *Annu. Rev. Med.* **50**, 87–98
- Garcia, K. C., Teyton, L., and Wilson, I. A. (1999) *Annu. Rev. Immunol.* **17**, 369–397
- Lebrón, J. A., Bennett, M. J., Vaughn, D. E., Chirino, A. J., Snow, P. M., Mintier, G. A., Feder, J. N., and Bjorkman, P. J. (1998) *Cell* **93**, 111–123
- Lawrence, C. M., Ray, S., Babyonyshev, M., Galluser, R., Borhani, D. W., and Harrison, S. C. (1999) *Science* **286**, 779–782
- Bennett, M. J., Lebrón, J. A., and Bjorkman, P. J. (2000) *Nature* **403**, 46–53
- Lebrón, J. A., West, A. P., and Bjorkman, P. J. (1999) *J. Mol. Biol.* **294**, 239–245
- Kawabata, H., Yang, R., Hiramata, T., Vuong, P. T., Kawano, S., Gombart, A. F., and Koeffler, H. P. (1999) *J. Biol. Chem.* **274**, 20826–20832
- Kawabata, H., Germain, R. S., Vuong, P. T., Nakamaki, T., Said, J. W., and Koeffler, H. P. (2000) *J. Biol. Chem.* **275**, 16618–16625
- Fleming, R. E., Migas, M. C., Holden, C. C., Waheed, A., Britton, R. S., Tomatsu, S., Bacon, B. R., and Sly, W. S. (2000) *Proc. Natl. Acad. Sci. U. S. A.* **97**, 2214–2219
- Camaschella, C., Roetto, A., Cali, A., De Gobbi, M., Garozzo, G., Carella, M., Majorano, N., Totaro, A., and Gasparini, P. (2000) *Nat. Genet.* **25**, 14–15
- Fägerstam, L. G., Frostell-Karlsson, A., Karlsson, R., Persson, B., and Rönnber, I. (1992) *J. Chromatogr.* **597**, 397–410
- Malmqvist, M. (1993) *Nature* **361**, 186–187
- Morton, T. A., and Myszkka, D. G. (1998) *Methods Enzymol.* **295**, 268–294
- Ramalingam, T. S., West, A. P., Lebrón, J. A., Nangiana, J. S., Hogan, T. H., Enns, C. A., and Bjorkman, P. J. (2000) *Nat. Cell Biol.*, in press
- Dubljevic, V., Sali, A., and Goding, A. (1999) *Biochem. J.* **341**, 11–14
- Riedel, H. D., Muckenthaler, M. U., Gehrke, S. G., Mohr, I., Brennan, K., Herrmann, T., Fitscher, B. A., Hentze, M. W., and Stremmel, W. (1999) *Blood* **94**, 3915–3921
- Jones, S., and Thornton, J. M. (1996) *Proc. Natl. Acad. Sci. U. S. A.* **93**, 13–20